PCCP

Accepted Manuscript

This article can be cited before page numbers have been issued, to do this please use: S. Sahu, M. Das, A. K. Bharti and G. Krishnamoorthy, *Phys. Chem. Chem. Phys.*, 2018, DOI: 10.1039/C8CP03835J.

ROYAL SOCIETY OF CHEMISTRY

rsc.li/pccp

View Article Online
DOI: 10.1039/C8CP03835J

Proton Transfer Triggered Proton Transfer: A Self-Assisted Twin Excited State Intramolecular Proton Transfer[§]

Saugata Sahu, Minati Das, Aditya Kumar Bharti, G. Krishnamoorthy[*]

Department of chemistry, Indian Institute of Technology Guwahati, Guwahati, Assam 781039, India.

Corresponding Author,

*Email: gkrishna@iitg.ernet.in

[§]Dedicated to Professor Jack Saltiel on his 81[st] birthday.

View Article Online
DOI: 10.1039/C8CP03835J

ABSTRACT. Double excited state intramolecular proton transfer (ESIPT) of 3,5-bis(2-hydroxyphenyl)-1H-1,2,4-triazole (bis-HPTA), a molecule possessing two intramolecular hydrogen bonded donor-acceptor pairs, has been investigated. The molecule undergoes not only a single ESIPT, but also the rare twin ESIPT. The most interesting fact is that initially, only one acid-base pair is ESIPT active and the other pair is ESIPT inactive. The first proton transfer triggers the proton transfer in the second acid-base pair by creating an appropriate condition. This new class of sequential proton transfer is labeled as 'proton transfer triggered proton transfer' (PTTPT). The PTTPT has been demonstrated with steady state and time resolved fluorescence techniques. It was further substantiated by the theoretical data and using a chemically modified system (3-(2-hydroxyphenyl)-5-(2-methoxyphenyl)-1H-1,2,4-triazole.

KEYWORDS: ESIPT, Double Proton Transfer, Cooperative Proton Transfer, Triazole, Annular Tautomer.

View Article Online
DOI: 10.1039/C8CP03835J

1. Introduction

Photoinduced proton transfer plays a fundamental role in several different chemical and biological processes[1-7] such as genetic mutation in the DNA base pair,[1] synthesis of ATP,[2] catalytic reduction of methionine sulfoxide to methionine.[3] The proton transfer may be an intermolecular or intramolecular process. Excited state intermolecular proton transfer has found many uses[8-12] for example in ratiometric sensing,[8, 9] pH indicating,[10] micro-environment probing,[11] photolithography.[12] The intramolecular proton transfer process has also drawn much attention in scientific research due to the potential applications of these molecules in laser dye,[13] solar concentrator,[14] photostabilizer,[15, 16] molecular data storage,[17] light emitting diode,[18] sensing,[19-22] probing[23].

Different types of photoinduced proton transfer have been reported. For example, 1-naphthol,[24] 2-hydroxynaphthalene-6-sulfonate,[25] 7-hydroxycoumarin,[26] luciferin[27] undergo solvent assisted excited state intermolecular proton transfer and produce anion in the excited state. The dimer of 7-azaindole exhibits a concerted intermolecular double proton transfer.[28] Most recently, a triple proton transfer mechanism was reported with a cyclic trimer of azaindole.[29] A solvent assisted relay proton transfer was observed in 7-hydroxyquinoline.[30] Weller first reported the excited state intramolecular proton transfer (ESIPT) which follows a four level cyclic process.[31] It occurs via the intramolecular hydrogen bond which is a prerequisite for ESIPT. Different proton donor-acceptor coupled ESIPT molecules lead to different kinds of tautomerism such as enol-keto, imine-amine, enol-amine, imine-keto. Most of these molecules follow a single proton transfer process in the excited state. Recently, the development of double/multiple intramolecular proton transfer systems has gained interest.[32-35] However, the chemical modification of a system with a

View Article Online
DOI: 10.1039/C8CP03835J

single ESIPT unit to a system with multiple ESIPT units often does not lead to a multiple proton transfer system.[34, 36-38] Upon photoexcitation the modified systems underwent single proton transfer rather than twin or multiple proton transfer. Chou and his co-workers reported intramolecular relay type double proton transfer with 7-hydroxyquinoline-8-carboxylic acid and 1,8-dihydroxy-2-naphthaldehyde.[32, 33] The interesting aspect of these systems is that the initial proton transfer is carried forward to another unit(s) in the excited state. The dual ESIPT systems have to undergo a twin proton transfer to generate a dual tautomerized state. The phenomenon is unusual and such systems are rarely reported.[32, 33, 35, 39, 40] A cooperative twin proton transfer upon photoexcitation were reported earlier in 2,5-bis(benzoxazol-2-yl)thiophene-3,4-diol,[40, 41] 2,2'-bipyridine-3,3'-diol and 2,2'-bipyridine-3,3'-diamine.[39, 42-44] The double proton transfer mechanism of 2,2'-bipyridine-3,3'-diol and 2,2'-bipyridine-3,3'-diamine are well established.[42, 43, 45-49] They comprised of two identical donor-acceptor units and show a sequential proton transfer which can commence from any of the donor-acceptor unit. Due to the fast proton transfer from the monoketo to the diketo, the steady state tautomer emission appears only from the diketo species of 2,2'-bipyridine-3,3'-diol and 2,2'-bipyridine-3,3'-diamine.

In the present work, we report a new class of proton transfer, proton transfer triggered proton transfer (PTTPT) in 3,5-bis(2-hydroxyphenyl)-1H-1,2,4-triazole (bis-HPTA, Chart 1A). bis-HPTA possesses two phenolic units (proton donor) attached with a 1,2,4-triazole unit (proton acceptor). The donor-acceptor systems in bis-HPTA (α and β, Chart 1) are not electronically identical and they should yield different keto forms upon photo-excitation. The first proton transfer (ESIPT-I) produces emission from mono keto tautomer. The second proton transfer (ESIPT-II) produces a different emission from a double tautomerized state. We observed that the ESIPT-I triggers the ESIPT-II. Otherwise ESIPT-II is not feasible in the solution. In system such

View Article Online
DOI: 10.1039/C8CP03835J

as 2,2'-bipyridine-3,3'-diol or diamine, ESIPT in both the donor-acceptor systems are feasible and equally probable. Thus, PTTPT of bis-HPTA produces a twin ESIPT emission by a rare twin ESIPT mechanism.

Chart 1. Molecular structures of (A) 3,5-bis(2-hydroxyphenyl)-1H-1,2,4-triazole (bis-HPTA), (B) 3-(2-hydroxyphenyl)-5-(2-methoxyphenyl)-1H-1,2,4-triazole (HPMPTA).

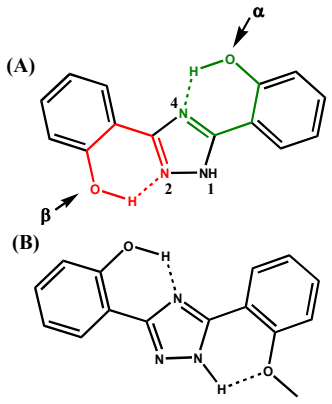

2. Materials and methods

bis-HPTA was prepared in two steps (Scheme S1A).[50] In the first step, 2-(2'-hydroxyphenyl)-4H-1,3-benzoxazin-4-one was synthesized by the reaction of equimolar amount of salicylic acid and salicylamide in the presence of thionyl chloride and a catalytic amount of pyridine in xylene. The purified product (by column chromatography) was reacted with an equivalent amount of hydrazine monohydrate in diethyl ether to yield the final product.

Bis-HPTA: white solid; ^{1}H NMR (600 MHz, DMSO-d_6) δ 11.46 (s, 2H), 8.02 (d, J = 7.8 Hz, 2H), 7.35 (m, J = 7.7 Hz, 2H), 7.03 (d, J = 8.1 Hz, 2H), 7.00 (m, 2H) (Figure S1, ESI). ^{13}C NMR (600 MHz, DMSO) δ 155.90, 131.36, 127.52, 119.52, 116.61, 113.42. (two carbons did not appear, Figure S2, ESI). HRMS (M+1) 254.093 (254.093 cal.).

View Article Online
DOI: 10.1039/C8CP03835J

The mono-methoxy derivative of bis-HPTA, 3-(2-hydroxyphenyl)-5-(2-methoxyphenyl)-1H-1,2,4-triazole (HPMPTA) was synthesized in a two step process (Scheme S1B). First, 2-hydroxy-N-(2-methoxybenzoyl)benzamide (HMBB) was synthesized by the reaction of an equimolar amount of salicylamide and 2-methoxybenzoicacid in the presence of thionyl chloride and a catalytic amount of pyridine in xylene. It was purified with column chromatography. Benzamide 1 mmole, hydrazine hydrate 1 mmole were added to 3 mL 30% acetic acid and the solution was refluxed at 118° C for 24 h. A clear solution was observed at the end of the reaction. It was partially neutralized with 2% sodium bicarbonate solution. The product was extracted with chloroform and purified by column chromatography. HPMPTA was characterized with ^{1}H NMR, ^{13}C NMR and HRMS.

HMBB: pale yellow solid; ^{1}H NMR (600 MHz, DMSO-d_6) δ 7.89 (d, J = 7.9 Hz, 1H), 7.83 (d, J = 7.7 Hz, 1H), 7.58 (m, 1H), 7.44 (m, 1H), 7.21 (d, J = 8.4 Hz, 1H), 7.10 (m, 1H), 7.03 (d, J = 8.2 Hz, 1H), 6.96 (m, 1H), (Figure S3, ESI). HRMS (M+1) 272.093 (272.093 cal.).

HPMPTA: white solid; ^{1}H NMR (600 MHz, $CDCl_3$): δ 12.21 (s, 1H), 11.28 (s, 1H), 8.28 (d, J = 7.7 Hz, 1H), 8.10 (d, J = 7.7 Hz, 1H), 7.46 (m, 1H), 7.30 (m, 1H), 7.17 (m, 1H), 7.04 (d, J = 8.2 Hz, 1H), 6.99 (d, J = 8.3 Hz, 1H), 6.92 (m, 1H), 3.94 (s, 3H) (Figure S4, ESI). ^{13}C NMR (600 MHz, $CDCl_3$) δ 160.80, 157.28, 157.02, 152.08, 132.35, 131.15, 129.78, 126.87, 121.92, 119.52, 117.38, 114.47, 111.47, 56.12, (Figure S5, ESI). HRMS (M+1) 268.108 (268.109 cal.).

All the required chemicals for the synthesis were purchased from Sigma Aldrich, USA. All solvents were purchased from Spectrochem, India.

The absorption spectra were recorded with a Perkin Elmer Lambda 750 UV-Visible spectrometer. The steady state emission and excitation spectra were acquired using a Horiba

View Article Online
DOI: 10.1039/C8CP03835J

Fluoromax-4 spectrometer. HPLC grade solvents were used for spectral studies. The concentration of dyes was 5 μM for all photophysical experiments. The fluorescence quantum yields were measured using quinine sulphate solution in 1 N sulphuric acid (φ_f = 0.55) as reference.[51] Edinburgh instrument LifeSpec-II was used to record the fluorescence lifetime with a Hamamatsu MCP detector with response time of ~ 300 ps for the rising time and ~ 500 ps for the decay time. A 308 nm LED light sources with full width at half maximum 635 picosecond was used for the lifetime measurement. The pulse repetition rate was adjusted to 5 MHz. The time-resolved emission spectra were constructed using the method reported by Koti et al.[52]

Theoretical calculations were performed using Gaussian 09W program to obtain different molecular parameters.[53] GaussView 5.0 was used to draw the molecular structures, to obtain the coordinates and to feed the inputs. The density functional theory (DFT)[54, 55] and the time dependent DFT (TDDFT) were used to optimize the ground and the excited state geometries, respectively.[56] A 6-31+G(d,p) basis set with Becke's three-parameter exchange functional along with Lee-Yang-Parr nonlocal correlation functional (B3LYP) was used for the geometry optimization.[57, 58] The excitation and the emission energies were calculated from the optimized ground state and excited state geometries, respectively using TDDFT/B3LYP/6-31+G(d,p) calculations.[59] The solvent stabilization of the molecule was included by using integral equation formalism-polarizable continuum model (IEF-PCM) and choosing tetrahydro furan (THF) as solvent. [60]

3. Results and discussion

3.1. Intrinsic photophysics of bis-HPTA and twin keto-emission

View Article Online
DOI: 10.1039/C8CP03835J

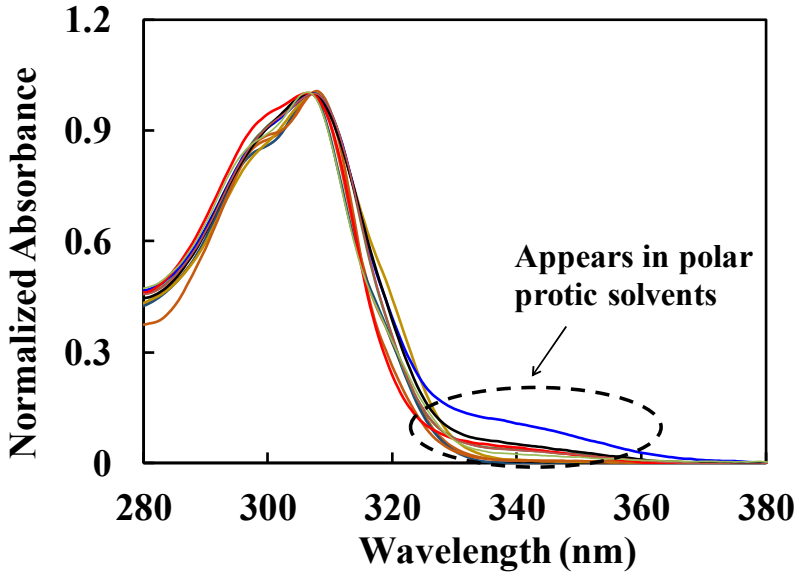

Figure 1. Normalized absorption spectra of bis-HPTA in different solvents.

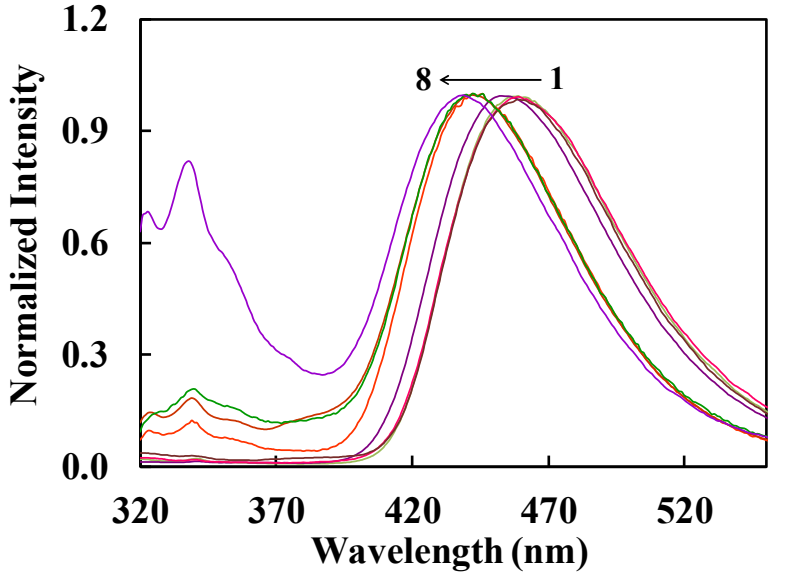

Figure 2. Normalized emission spectra of bis-HPTA in different solvents 1) ethyl acetate, 2) tetrahydrofuran, 3) dioxane, 4) chloroform, 5) 1-butanol, 6) 1-propanol, 7) 2-propanol, 8) methanol. λ_{ex} = 308 nm.

Figure 1 shows the absorption spectra of bis-HPTA in different solvents. The absorption maximum of bis-HPTA appears at ~ 308 nm and it shows a weak dependency on solvent polarity. The molecule possesses a high molar extinction co-efficient (2 x 10^4 $M^{-1}cm^{-1}$, in methanol). The vibrational structure of the absorption spectrum slowly blurs with increasing

View Article Online
DOI: 10.1039/C8CP03835J

solvent polarity. In polar protic solvents, along with the main absorption band a small band also appears around 340 nm (Figure 1). Upon excitation, depending on the solvent, a less Stokes shifted UV emission and a highly Stokes shifted visible emission are observed (Figure 2 and Table 1). In low polarity media such as cyclohexane, chloroform, tetrahydrofuran, dioxane, only the visible emission appears. The Stokes shift of the visible emission is as large as 11,000 cm^{-1}. The emission quantum yield is 0.04-0.08 in those solvents. With increasing solvent polarity, the visible emission gradually shifts toward the shorter wavelength. The ratio of the shorter wavelength emission band to the longer wavelength emission band gradually increases with hydrogen bond forming ability of solvent. In a solvent such as ethyl acetate, the ratio is 0.01. But, in a highly polar protic solvent such as methanol, the intensity ratio is 0.8. The Stokes shift of the UV emission in methanol is 3100 cm^{-1}. The less Stokes shifted UV emission suggests that it is the normal emission from the enol tautomer. The highly Stokes shifted visible emission exhibits a characteristic negative solvatochromic effect of the tautomer emission,[61, 62] and is therefore attributed to the emission from the keto species.

The proton transfer occurs from the phenolic unit to the triazole nitrogen of bis-HPTA molecule via the intramolecular hydrogen bond. In protic solvents, the intramolecular hydrogen bond is interrupted by the formation of intermolecular hydrogen bonds with solvent. The breaking of the intramolecular hydrogen bond results in the formation of solvated open conformer (see later) where the ESIPT is not feasible. Thus, results in the normal emission (340 nm emission). The excitation spectra also suggest the presence of two different conformers (see later). The fluorescence lifetime of bis-HPTA was recorded at normal and tautomer emission maxima in different solvents (Table 1, Figure 3). The excited enol and keto tautomer of imidazole-based ESIPT systems have fluorescence lifetimes of ~ 1.5 ns and ~ 3.5 ns,

View Article Online
DOI: 10.1039/C8CP03835J

respectively.[63-65] Apart from these two fluorescence lifetimes, another emission lifetime is observed when the tautomer emission of bis-HPTA was monitored (Table 1). It indicates the existence of more than one keto tautomer in the excited state.

Table 1. Absorption maxima (λ_{max}^{abs}, nm) emission maxima (λ_{max}^{em}, nm) and fluorescence lifetime (τ, ns)[a] of bis-HPTA in different solvents, λ_{ex} = 308 nm.

Solvent	λ_{max}^{abs}	λ_{max}^{em}	τ [b]	τ [c]
Ethyl acetate	307	460		0.7 (72)
				3.7 (28)
Dioxane	308	460		0.8 (61)
				3.9 (39)
Tetrahydrofuran	308	459		0.8 (62)
				4.0 (38)
Methanol	307	340, 438	1.4	0.7 (48)
			(100)	3.0 (52)
1-Propanol	308	340, 442	1.6	1.8 (70)
			(100)	4.1 (30)
1-Butanol	308	340, 444	1.6	2.4 (68)
			(100)	4.0 (32)

View Article Online
DOI: 10.1039/C8CP03835J

[a]Relative amplitude (in %) of different emitting species are given in parenthesis. [b]Emission monitored at shorter λ_{max}^{em}. [c]Emission monitored at longer λ_{max}^{em}.

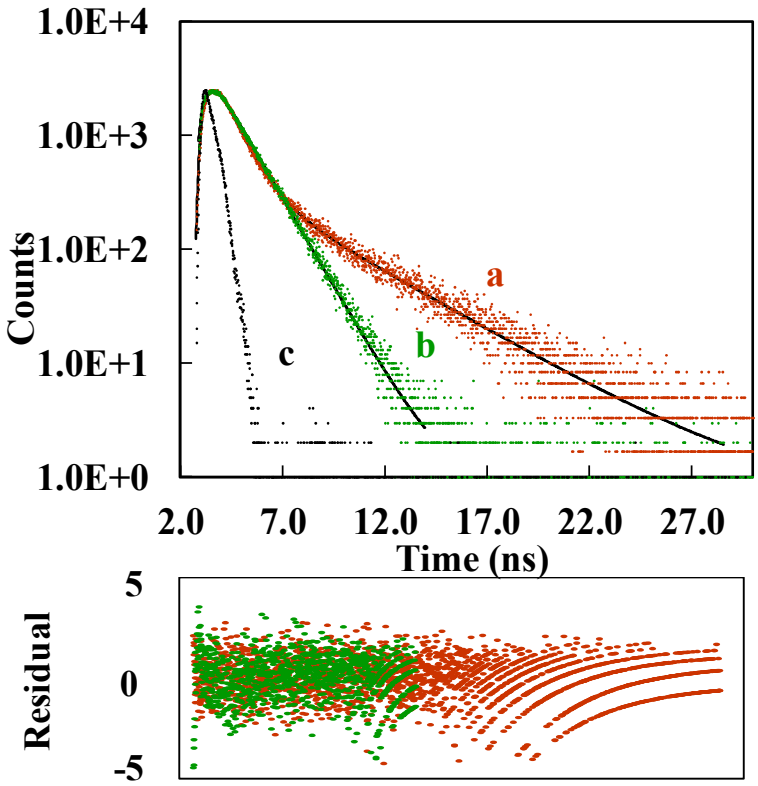

Figure 3. Fluorescence decays of (a) tautomer emission in dioxane (recorded at 460 nm) and (b) normal emission in methanol (recorded at 350 nm) and (c) the instrument response function, λ_{ex} = 308 nm. The corresponding residual plots are shown below the decay profile.

View Article Online
DOI: 10.1039/C8CP03835J

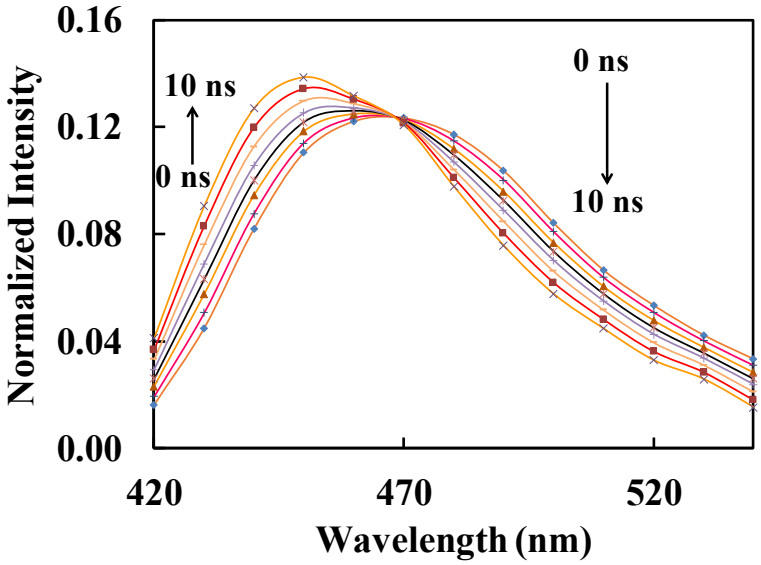

Figure 4. Time resolved area normalized emission spectra of bis-HPTA in dioxane obtained at different times 0 ns, 0.8 ns, 1.4 ns, 1.8 ns, 2.2 ns, 2.8 ns, 3.5 ns and 10 ns. λ_{ex} = 308 nm.

To obtain a better insight on the spectral-nature of the dual keto emission, time resolved area normalized emission spectra (TRANES) were constructed in dioxane where the interference from the enol emission is negligible. TRANES reveal the existence of two different emission bands with an isoemissive point. The emission maxima appear at 455 nm and 465 nm (Figure 4). The 455 nm emission is associated to 3.9 ns lifetime species and the 465 nm emission is associated with a 0.8 ns lifetime species. The traces of decays are shown in Figure S6. All decays were fitted well with two components emission decay (Table S1).

3.2 Role of ground state conformers

Scheme 1. Different possible conformers of bis-HPTA.

View Article Online
DOI: 10.1039/C8CP03835J

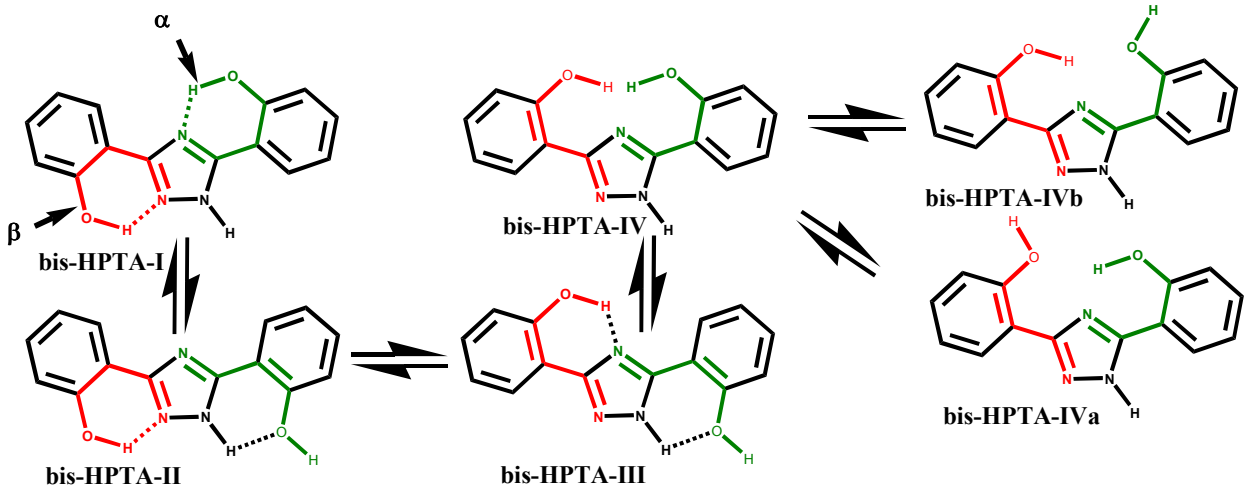

Table 2. Relative ground state energy of different bis-HPTA conformers with respect to bis-HPTA-I in THF.

Conformer	Relative Energy (eV)
bis-HPTA-I	0.000
bis-HPTA-II	0.113
bis-HPTA-III	0.083
bis-HPTA-IV	0.119
bis-HPTA-IVa	0.301
bis-HPTA-IVb	0.294

bis-HPTA has two phenolic units. The -OH groups of the phenolic units form intramolecular hydrogen bonds with the triazole nitrogens. The two six membered cyclic structures formed

View Article Online
DOI: 10.1039/C8CP03835J

through intramolecular hydrogen bonds differ from each other by the nitrogen that is involved in the hydrogen bond. We labeled them as α (colored in green) and β (colored in red) (Scheme 1). α involves the nitrogen that is attached to two carbon atoms. β involves the nitrogen that is attached to a carbon atom and a nitrogen atom. The torsional rotation results in different conformers (Scheme 1). However, due to the presence of strong intramolecular hydrogen bonds, the bis-HPTA-I would be the most stable conformer. The ground state geometries of different conformers of bis-HPTA were optimized (Table S2-S7, ESI). Theoretical calculations also support that the bis-HPTA-I conformer is the most stable conformer (Table 2). The Boltzmann populations contribution of other conformers at ambient temperature are less than 2% compared to bis-HPTA-I. The calculated lowest excitation energy of bis-HPTA-I in tetrahydrofuran is 305 nm and it agrees well with the experimental value. The 'O-H' bond lengths in α and β are 0.99 Å and 0.98 Å, respectively. The distances between the acidic proton and the receptor sp^2 nitrogen are 1.75 Å and 1.80 Å in α and β, respectively. Thus, it appears that the intramolecular hydrogen bond in the α ring is stronger than in the β ring.

Scheme 2. Conformer in the protic solvents.

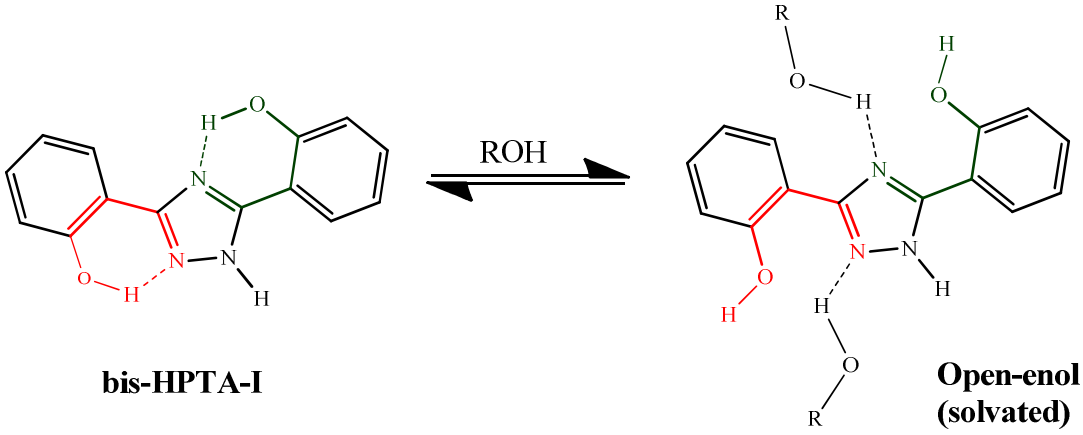

View Article Online
DOI: 10.1039/C8CP03835J

Excitation spectra were recorded at different wavelengths of the visible emission (Figure 5). The complete overlapping of the excitation spectra suggests that both visible emissions originate from the same ground state precursor. It further rules out the formation of two different keto through the ESIPT of two different conformers. We recorded the excitation spectra in polar protic solvent also, to understand the origin of the enol emission (Figure S7, ESI). The excitation spectra recorded at 350 nm and 460 nm of bis-HPTA-I emission in methanol are not identical. This is consistent with the presence two different conformers, bis-HPTA-I and open-enol (Scheme 2). The formation of strong intermolecular hydrogen bond in protic solvents also facilitates the formation of anion through the intermolecular proton transfer in the ground state.[61] The weak absorbance/excitation band at ~ 340 nm observed in polar protic solvents may be due to the formation of anion (Figure 1, Figure S7, ESI). To verify our prediction, bis-HPTA was deprotonated further to form anion by adding sodium hydroxide to the methanol solution. The emission maximum of the anion appears at 400 nm and matches with the maximum of the emission band obtained upon excitation at 340 nm in methanol and other polar protic solvents (Figure S8, ESI). The absorption spectrum of the alkaline solution also has band at ~ 340 nm (ESI, Figure S8).

View Article Online
DOI: 10.1039/C8CP03835J

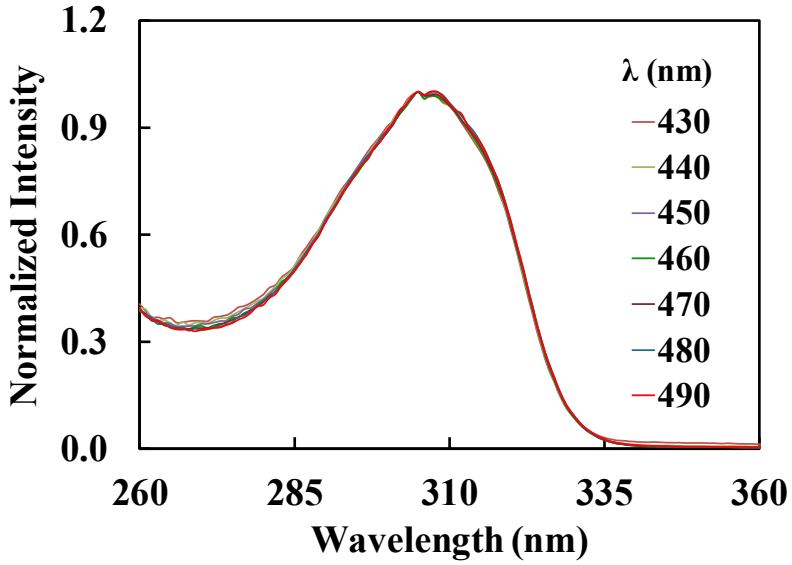

Figure 5. The normalized excitation spectra of bis-HPTA in dioxane, recorded at different emission wavelengths (λ).

3.3. The dual ESIPT and the pathway for the diketo tautomer.

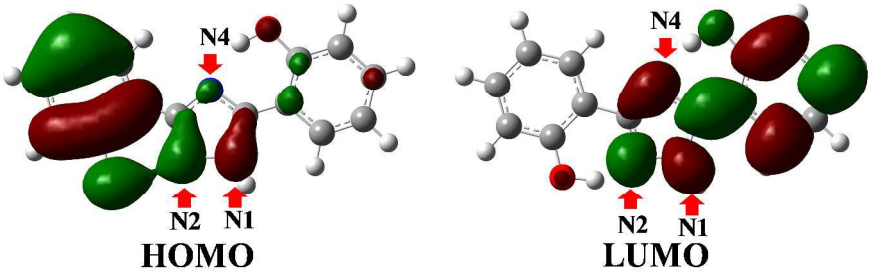

Figure 6. HOMO and LUMO of bis-HPTA-I, calculated in tetrahydrofuran.

Scheme 3. Plausible ways of single and dual ESIPT in bis-HPTA in the excited state.

View Article Online
DOI: 10.1039/C8CP03835J

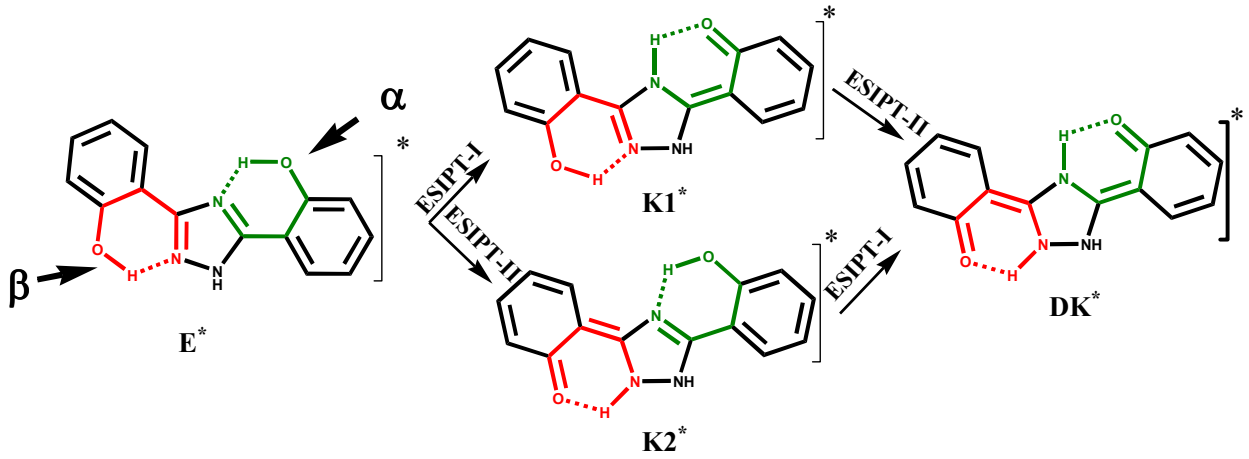

Table 3. Theoretically calculated energies[a] (eV) and emission energies (eV) of different keto forms in THF.

Species	Excited state	Corresponding Franck Condon ground state	Emission energy[b]	Oscillator strength (*f*)
K1	3.725	0.858	2.867 (2.723)	0.33
K2	3.411	1.361	2.050	0.07
DK	4.180	1.850	2.330 (2.667)	0.23

[a]The energies are relative energies with respected enol (bis-HPTA-I). [b]The values in parenthesis are experimental values.

Since bis-HPTA-I is the most stable conformer with strong intramolecular hydrogen bonds, the ESIPT should occur from bis-HPTA-I. The HOMO-LUMO corresponding to the longest wavelength electronic transition of bis-HPTA-I is given in Figure 6. Compared to the HOMO, the electron density on the acceptor triazole unit increases in the LUMO. Among the proton receptors, the N4 atom in the α ring becomes more electron rich than N2 in the β ring. The ESIPT processes in α and β rings are labeled as ESIPT-I and ESIPT-II, respectively (Scheme 3). The ESIPT-I, the ESIPT in α ring, will produce K1 tautomer. Similarly, ESIPT-II, the ESIPT in β ring will produce K2 tautomer. In K1 tautomer conjugation is within one of the donor-accepor unit, but in K2 the conjugation is more and it is extended over the entire molecule (Chart S1). TRANES reveal that both the keto emission maxima differ by small extent 455 nm and 465 nm (Figure 4). This indicates that the second keto emission is not from K2. The proton transfer in

View Article Online
DOI: 10.1039/C8CP03835J

the β ring (ESIPT-II) of the K1 tautomer yields a double tautomerized diketo (DK) tautomer (Scheme 3). In DK though the conjugation is present in both the of the donor-accepor units, but unlike in K2 they are separated. Therefore, the emission maximum of DK is expected to differ less that of K1 than the emission maximum of K2. To confirm further the keto tautomers, K1, K2 and DK of bis-HPTA were fully optimized in the excited state using THF as solvent (Table S8-S11). The theoretically calculated emission energy of K2 is less than that of DK which is less than that of K1 (Table 3). The theoretical transition energies of K1 and DK are compared with the experimental energies (Table 3) and there is a good agreement between theoretical and experimental emission energies. Therefore, the two-keto emissions in the visible region correspond to the emissions from K1 and DK. This is also consistent with the existence of the isoemissive point in the TRANES. It is a rare consecutive twin ESIPT process that produced the DK tautomer. To further substantiate the twin ESIPT process, the mono methylated derivative of bis-HPTA, HPMPTA (Chart 1) was designed and synthesized. HPMPTA produces a tautomer emission at 450 nm (Figure S9). Unlike those of bis-HPTA, the tautomer emission of HPMPTA exhibits a mono-exponential decay with a fluorescence lifetime of 4.5 ns in dioxane. This substantiates the conclusion. The probable excited paths of the excited bis-HPTA-I is shown Scheme 4. Upon excitation, enol is excited to the Frank-Condon state (a higher vibrational level) of the excited electronic state. The ESIPT process is an ultrafast process.[33, 66] The absence of enol emission in nonpolar solvents suggest that ESIPT-I occurs faster than the vibrational relaxation to produce K1. It appears that ESIPT-II competes with vibrational relaxation of K1. Therefore, the emissions observed from both K1* and DK*. The proton transfers and vibrational relaxations are seemed to be faster than our instrument's response time therefore no rising components are observed for K1* and DK*. Since the ESIPT processes occur from higher

View Article Online
DOI: 10.1039/C8CP03835J

vibrational state and the emission occurs from the relaxed vibration state (v = 0 state of the first electronic excited state), the fluorescence lifetimes obtained are the corresponding lifetime of the emitting states. In ESIPT molecules, torsional rotation of the phenyl ring of the keto tautomer in the excited state is reported as a possible path of de-excitation.[64, 65, 67, 68] The K1* has one such possibility, but DK* has two such possibilities. This may be the cause of the shorter lifetime of DK* as compared to that of K1*.

View Article Online
DOI: 10.1039/C8CP03835J

Scheme 4. The plausible excited state processes of excited enol of bis-HPTA in THF along with the calculated, (relative) energies, transition energies and the oscillator strengths (*f*). The transition energies and lifetime in parenthesis are experimental values. Corresponding Franck Condon states are denoted as FC state

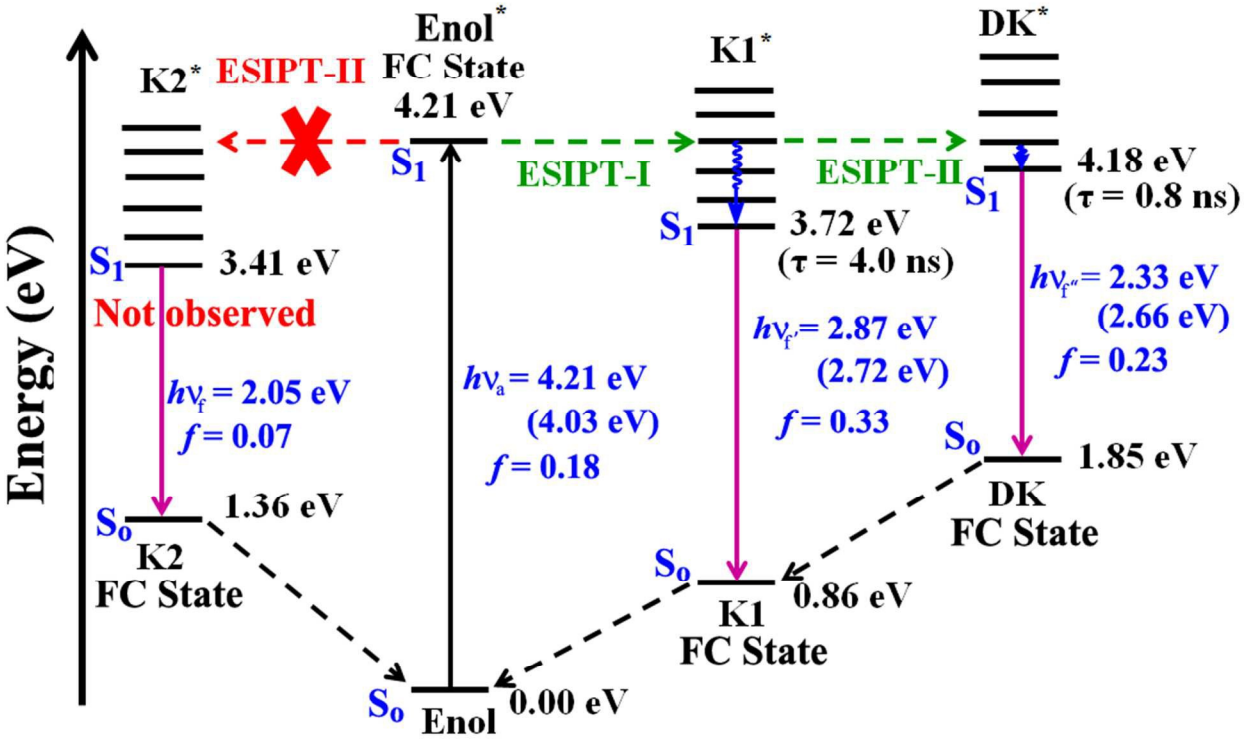

3.4. Annular tautomerism and proton transfer triggered proton transfer

The absence of K2 emission in solution indicates that the ESIPT process through β unit (red in color, Scheme 2) is prevented by some factor in the solution. This anomalous behavior of the molecule can be explained with the annular tautomerism that takes place between N1-H and N2 of the triazole system (Scheme 3).[69-73] Due to the presence of electron withdrawing sp^2 nitrogen (N2 and N4), the N1-H proton in the azole ring is fairly acidic and the proton is being shared between N1 and N2.[74, 75] The mobility of the N-H proton in 1,2,4-triazole also produces extra stabilization through aromatization.[76] The intramolecular hydrogen bond in the β unit is strongly perturbed due to this shuttling of the acidic proton. The shifting of the proton from N1 to N2 provides a less stable tautomer than bis-HPTA-I, which is basically the bis-HPTA-III conformer

View Article Online
DOI: 10.1039/C8CP03835J

(Scheme 4 and Scheme 1). Eventually, this annular tautomer would switch back to the more stable bis-HPTA-I conformer by the torsional rotation of the phenyl rings (Scheme 4). Therefore, in solution, β ring is weakened and fails to commence the ESIPT-II process. However, after the first proton transfer (when the proton is transferred to N4), the acidity of N1-H decreases and the efficiency of the annular tautomerism also diminishes. It facilitates the ESIPT-II in β. Thereby, the ESIPT-I triggers the ESIPT-II. We named this new class of proton transfer as 'proton transfer triggered proton transfer' (PTTPT). In PTTPT a proton transfer, which is otherwise not viable, is made feasible by the other proton transfer. In bis-HPTA, the ESIPT-II is blocked because of annular tautomerism. The ESIPT-I weakened the annular tautomerism, thereby strengthened the intramolecular hydrogen bond in the β ring. This facilitates and triggers the ESIPT-II. Therefore, in bis-HPTA the PTTPT is a self-assisted twin ESIPT processes. Unlike in relay proton transfer where the proton acceptor which donates the proton in subsequent steps, in this PTTPT the proton acceptor in the first step is not donating the proton in the second step. The first proton transfer aided the (otherwise not feasible) second proton transfer. All these make this PTTPT a unique class of proton transfer.

Scheme 4. Annular tautomerism and conformational equilibrium of bis-HPTA in solution.

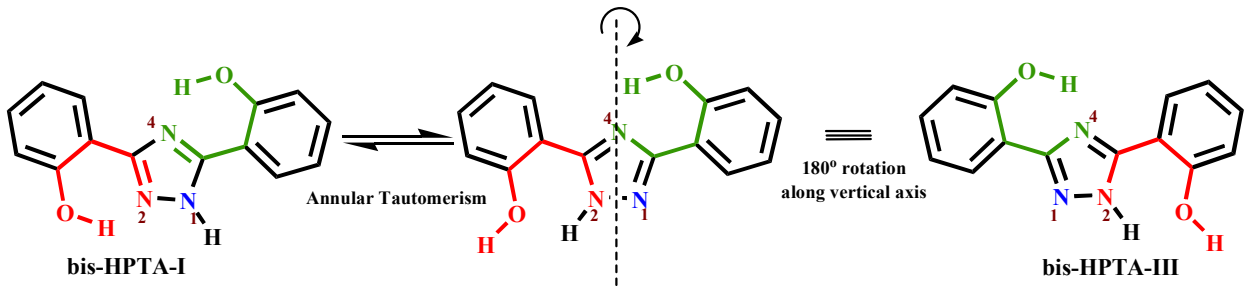

3.5. Tautomer emissions in the powder sample

View Article Online
DOI: 10.1039/C8CP03835J

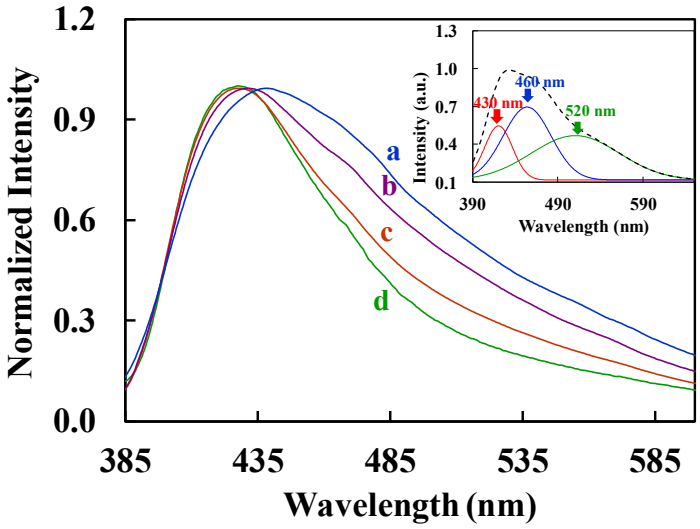

Figure 7. Emission spectra of bis-HPTA powder at different excitation wavelengths (a) 340 nm, (b) 350 nm, (c) 360 nm, (d) 370 nm. The spectrum 'a' was deconvoluted intro three gaussian spectra (inset).

In solution medium, the ESIPT cannot be initiated in β ring due to annular tautomerism and it takes place only after the occurrence of the ESIPT-I. Such a fast exchange of proton by annular tautomerism may reduce in the solid. Therefore, we studied the ESIPT process of bis-HPTA with powder sample. In powder sample, a longer wavelength emission appears at ~520 nm along with other emissions (Figure 7). The emission maximum recorded for the powder sample is excitation wavelength dependent. The wavelength dependency of the emission spectra indicates the existence of multiple ground state species. However, our interest mainly lies on the appearance of the longest wavelength emitting species. A triexponential fluorescence decay with lifetime 4.0 ns, 0.3 ns and 1.1 ns is obtained for the emission monitored at 430 nm, 460 nm and 520 nm (Table 4). The relative population of 1.1 ns lifetime species increases when monitored at longer wavelength. The longest wavelength emitting species with fluorescence lifetime 1.1 ns does not appear in solution. This longest wavelength emission can appear only if the ESIPT

View Article Online
DOI: 10.1039/C8CP03835J

process is initiated in β ring not in the other ring. In solid state, due to the structural rigidity the torsional rotation and the annular tautomerism may have been reduced. Subsequently, in solid state, the proton may be more localized on N1 nitrogen, and ESIPT-II also commenced in β ring directly from the enol form. Therefore, not as in the solution, K2 species is also present along with K1 and DK in the powder sample. The shortening of lifetime to 0.3 ns may be due to aggregation induced quenching and the molecular aggregation is reported to enhance the intersystem crossing in some molecules.[77-80]

Table 4. Emission lifetime of bis-HPTA powder recorded at different emission wavelengths (λ). λ_{ex} = 336 nm. Relative population is provided in the parenthesis.

λ (nm)	τ_1 (ns)	τ_2 (ns)	τ_3 (ns)	χ^2
430	0.3 (34)	1.1 (35)	4.0 (31)	0.95
460	0.3 (49)	1.1 (27)	4.0 (24)	1.00
520	0.3 (37)	1.1 (43)	4.0 (20)	0.94

4. Conclusion.

We have reported a new kind of proton transfer 'proton transfer triggered proton transfer'. It is a twin ESIPT in which two consecutive ESIPT produce a dual keto tautomer, DK. In bis-HPTA both the protons are transferred from different ring to the acceptors in the same ring i.e. the triazole. In solution the process is initiated first in the α ring. The ESIPT process cannot commence from the other phenolic unit due to the annular tautomerism. After the first proton transfer, ESIPT-I, the acidity of the N1-H proton decreases and the second ESIPT, ESIPT-II takes place. However, in solid sample, due to the structural rigidity annular tautomerism is not efficient enough, and both the phenol unit undergoes ESIPT. Due to the structural resemblance, the emission maxima of the K1 (monoketo) and the DK species are close to each other. The experimental findings are supported well by the theoretical predictions.

View Article Online
DOI: 10.1039/C8CP03835J

Electronic Supplementary Information (ESI). NMR spectra of bis-HPTA, HMBB, HPMPTA. Excitation spectra of bis-HPTA in methanol. Emission and fluorescence decay of HPMPTA in dioxane. Anionic emission of bis-HPTA. XYZ co-ordinates of different ground and excited tautomer.

ACKNOWLEDGMENT

The authors acknowledge Central Instruments Facility, IIT Guwahati. Saugata Sahu thanks the Council of Scientific and Industrial Research, India for the fellowship. The authors thank Professor Jack Saltiel, Florida State University for his valuable comments and suggestions.

REFERENCES

1. O. K. Abou-Zied, R. Jimenez and F. E. Romesberg, *J. Am. Chem. Soc.*, 2001, **123**, 4613-4614.
2. T. Beke-Somfai, P. Lincoln and B. Nordén, *Proceedings of the National Academy of Sciences*, 2011, **108**, 4828-4833.
3. E. Thiriot, G. Monard, S. Boschi-Muller, G. Branlant and M. Ruiz-López, *Theor. Chem. Acc.*, 2011, **129**, 93-103.
4. Y. Fujii, M. Hata, T. Hoshino and M. Tsuda, *J. Phys. Chem. B*, 2002, **106**, 9687-9695.
5. M. De Vivo, B. Ensing and M. L. Klein, *J. Am. Chem. Soc.*, 2005, **127**, 11226-11227.
6. M. A. Rangelov, G. N. Vayssilov, V. M. Yomtova and D. D. Petkov, *J. Am. Chem. Soc.*, 2006, **128**, 4964-4965.
7. C.-G. Zhan, F. Zheng and D. W. Landry, *J. Am. Chem. Soc.*, 2003, **125**, 2462-2474.
8. X. Peng, Y. Wu, J. Fan, M. Tian and K. Han, *J. Org. Chem.*, 2005, **70**, 10524-10531.
9. X. Zhang, L. Guo, F.-Y. Wu and Y.-B. Jiang, *Org. Lett.*, 2003, **5**, 2667-2670.
10. K. Li, Q. Feng, G. Niu, W. Zhang, Y. Li, M. Kang, K. Xu, J. He, H. Hou and B. Z. Tang, *ACS Sens*, 2018, **3**, 920-928.
11. B. Cohen, C. M. Alvarez, N. A. Carmona, J. A. Organero and A. Douhal, *J. Phys. Chem. B*, 2011, **115**, 7637-7647.
12. L. G. Arnaut and S. J. Formosinho, *J. Photochem. Photobiol., A*, 1993, **75**, 1-20.
13. Z. Wei, Y. Yongli, G. Jianmin, Y. Jiannian and Z. Y. Sheng, *Angew. Chem. Int. Ed.*, 2015, **54**, 7125-7129.
14. D.-Y. Chen, C.-L. Chen, Y.-M. Cheng, C.-H. Lai, J.-Y. Yu, B.-S. Chen, C.-C. Hsieh, H.-C. Chen, L.-Y. Chen, C.-Y. Wei, C.-C. Wu and P.-T. Chou, *Acs. Appl. Mater. Inter.*, 2010, **2**, 1621-1629.
15. M. J. Paterson, M. A. Robb, L. Blancafort and A. D. DeBellis, *J. Phys. Chem. A*, 2005, **109**, 7527-7537.

View Article Online
DOI: 10.1039/C8CP03835J

16. P. Yang, J. Zhao, W. Wu, X. Yu and Y. Liu, *J. Org. Chem.*, 2012, **77**, 6166-6178.
17. S.-J. Lim, J. Seo and S. Y. Park, *J. Am. Chem. Soc.*, 2006, **128**, 14542-14547.
18. K.-C. Tang, M.-J. Chang, T.-Y. Lin, H.-A. Pan, T.-C. Fang, K.-Y. Chen, W.-Y. Hung, Y.-H. Hsu and P.-T. Chou, *J. Am. Chem. Soc.*, 2011, **133**, 17738-17745.
19. S. Freire, F. Rodriguez-Prieto, M. C. Rios Rodriguez, J. C. Penedo, W. Al-Soufi and M. Novo, *Chem. - Eur. J.*, 2015, **21**, 3425-3434.
20. Y. Venkatesh, J. Das, A. Chaudhuri, A. Karmakar, T. K. Maiti and N. D. P. Singh, *Chem. Commun.*, 2018, **54**, 3106-3109.
21. B. Shrabani, M. S. K., B. Sandipan, N. Surajit, G. Moumita, D. Satyahari, A. Anakuthil and P. S. N. D., *Angew. Chem. Int. Ed.*, 2016, **55**, 4194-4198.
22. F. A. S. Chipem, S. K. Behera and G. Krishnamoorthy, *Sensors and Actuators B: Chemical*, 2014, **191**, 727-733.
23. X. Li, R.-R. Tao, L.-J. Hong, J. Cheng, Q. Jiang, Y.-M. Lu, M.-H. Liao, W.-F. Ye, N.-N. Lu, F. Han, Y.-Z. Hu and Y.-H. Hu, *J. Am. Chem. Soc.*, 2015, **137**, 12296-12303.
24. O. Gajst, L. Pinto da Silva, J. C. G. Esteves da Silva and D. Huppert, *J. Phys. Chem. A*, 2018, **122**, 4704-4716.
25. P. Krishnakumar, R. Kar and D. K. Maity, *J. Phys. Chem. A*, 2018, **122**, 929-936.
26. J. Seixas de Melo and P. F. Fernandes, *J. Mol. Struct.*, 2001, **565-566**, 69-78.
27. I. Presiado, Y. Erez and D. Huppert, *J. Phys. Chem. A*, 2010, **114**, 9471-9479.
28. R. Crespo-Otero, N. Kungwan and M. Barbatti, *Chem. Sci.*, 2015, **6**, 5762-5767.
29. T.-H. Tu, Y.-T. Chen, Y.-A. Chen, Y.-C. Wei, Y.-H. Chen, C.-L. Chen, J.-Y. Shen, Y.-H. Chen, S.-Y. Ho, K.-Y. Cheng, S.-L. Lee, C.-h. Chen and P.-T. Chou, *Angew. Chem. Int. Ed.*, 2018, **57**, 5020-5024.
30. M. Itoh, T. Adachi and K. Tokumura, *J. Am. Chem. Soc.*, 1984, **106**, 850-855.
31. A. Weller, *Naturwissenschaften*, 1955, **42**, 175-176.
32. C.-Y. Peng, J.-Y. Shen, Y.-T. Chen, P.-J. Wu, W.-Y. Hung, W.-P. Hu and P.-T. Chou, *J. Am. Chem. Soc.*, 2015, **137**, 14349-14357.
33. K.-C. Tang, C.-L. Chen, H.-H. Chuang, J.-L. Chen, Y.-J. Chen, Y.-C. Lin, J.-Y. Shen, W.-P. Hu and P.-T. Chou, *J. Phys. Chem. Lett.*, 2011, **2**, 3063-3068.
34. I. E. Serdiuk and A. D. Roshal, *Dyes Pigments*, 2017, **138**, 223-244.
35. K. C. G. Sreedevi, A. P. Thomas, K. H. Aparna, R. Pradhan, M. L. P. Reddy, U. Lourderaj and A. Srinivasan, *Chem. Commun.*, 2014, **50**, 8667-8669.
36. S. Park, J. E. Kwon, S. H. Kim, J. Seo, K. Chung, S.-Y. Park, D.-J. Jang, B. M. Medina, J. Gierschner and S. Y. Park, *J. Am. Chem. Soc.*, 2009, **131**, 14043-14049.
37. M. Tasior, V. Hugues, M. Blanchard-Desce and D. T. Gryko, *Chem. -Asian. J.*, 2012, **7**, 2656-2661.
38. J. Piechowska, K. Virkki, B. Sadowski, H. Lemmetyinen, N. V. Tkachenko and D. T. Gryko, *J. Phys. Chem. A*, 2014, **118**, 144-151.
39. H. Bulska, *Chem. Phys. Lett.*, 1983, **98**, 398-402.
40. H. M. Kim, H.-J. Choo, S.-Y. Jung, Y.-G. Ko, W.-H. Park, S.-J. Jeon, C. H. Kim, T. Joo and B. R. Cho, *ChemBioChem*, 2007, **8**, 553-559.
41. Y. Hao and Y. Chen, *Dyes Pigments*, 2016, **129**, 186-190.
42. J. M. Ortiz-Sánchez, R. Gelabert, M. Moreno and J. M. Lluch, *ChemPhysChem*, 2007, **8**, 1199-1206.
43. F. Plasser, M. Barbatti, A. J. Aquino and H. Lischka, *J. Phys. Chem. A*, 2009, **113**, 8490-8499.

View Article Online
DOI: 10.1039/C8CP03835J

44. H. Zhang, P. van der Meulen and M. Glasbeek, *Chem. Phys. Lett.*, 1996, **253**, 97-102.
45. J. Zhao, X. Liu and Y. Zheng, *J. Phys. Chem. A*, 2017, **121**, 4002-4008.
46. O. K. Abou-Zied, *J. Phys. Chem. B*, 2009, **114**, 1069-1076.
47. J. M. Ortiz-Sánchez, R. Gelabert, M. Moreno and J. M. Lluch, *ChemPhysChem*, 2010, **11**, 3696-3703.
48. J. M. Ortiz-Sánchez, R. Gelabert, M. Moreno, J. M. Lluch, J. M. Anglada and J. M. Bofill, *Chem. Eur. J.*, 2010, **16**, 6693-6703.
49. J. M. Ortiz-Sánchez, R. Gelabert, M. Moreno and J. M. Lluch, *ChemPhysChem*, 2008, **9**, 2068-2076.
50. S. Stucky, N. J. Koch, U. Heinz and K. Hegetschweiler, *Chem. Pap. - Chem. Zvesti*, 2008, **62**, 388-397.
51. G. A. Crosby and J. N. Demas, *J. Phys. Chem.*, 1971, **75**, 991-1024.
52. A. S. R. Koti, M. M. G. Krishna and N. Periasamy, *J. Phys. Chem. A*, 2001, **105**, 1767-1771.
53. M. J. Frisch, G. W. Trucks, H. B. Schlegel, G. E. Scuseria, M. A. Robb, J. R. Cheeseman, G. Scalmani, V. Barone, B. Mennucci, G. A. Petersson, H. Nakatsuji, M. Caricato, X. Li, H. P. Hratchian, A. F. Izmaylov, J. Bloino, G. Zheng, J. L. Sonnenberg, M. Hada, M. Ehara, K. Toyota, R. Fukuda, J. Hasegawa, M. Ishida, T. Nakajima, Y. Honda, O. Kitao, H. Nakai, T. Vreven, J. A. Montgomery Jr., J. E. Peralta, F. Ogliaro, M. J. Bearpark, J. Heyd, E. N. Brothers, K. N. Kudin, V. N. Staroverov, R. Kobayashi, J. Normand, K. Raghavachari, A. P. Rendell, J. C. Burant, S. S. Iyengar, J. Tomasi, M. Cossi, N. Rega, N. J. Millam, M. Klene, J. E. Knox, J. B. Cross, V. Bakken, C. Adamo, J. Jaramillo, R. Gomperts, R. E. Stratmann, O. Yazyev, A. J. Austin, R. Cammi, C. Pomelli, J. W. Ochterski, R. L. Martin, K. Morokuma, V. G. Zakrzewski, G. A. Voth, P. Salvador, J. J. Dannenberg, S. Dapprich, A. D. Daniels, Ö. Farkas, J. B. Foresman, J. V. Ortiz, J. Cioslowski and D. J. Fox, *Gaussian, Inc. Wallingford, CT, USA*, 2009.
54. P. Hohenberg and W. Kohn, *Phys. Rev.*, 1964, **136**, B864-B871.
55. W. Kohn and L. J. Sham, *Phys. Rev.*, 1965, **140**, A1133-A1138.
56. M. E. Casida, in *Recent Advances In Density Functional Methods: (Part I)*, World Scientific, 1995, pp. 155-192.
57. A. D. Becke, *J. Chem. Phys.*, 1993, **98**, 5648-5652.
58. C. Lee, W. Yang and R. G. Parr, *Phys. Rev. B*, 1988, **37**, 785-789.
59. E. K. U. Gross, J. F. Dobson and M. Petersilka, in *Density Functional Theory II*, ed. R. F. Nalewajski, Springer Berlin Heidelberg, 1996, vol. 181, ch. 2, pp. 81-172.
60. S. Miertuš, E. Scrocco and J. Tomasi, *Chem. Phys.*, 1981, **55**, 117-129.
61. F. Rodriguez-Prieto, J. Carlos Penedo and M. Mosquera, *J. Chem. Soc., Faraday Trans.*, 1998, **94**, 2775-2782.
62. S. Sahu, Ila, B. Shankar, M. Sathiyendiran and G. Krishnamoorthy, *J. Photochem. Photobiol., A*, 2018, **353**, 416-423.
63. A. Douhal, F. Amat-Guerri, M. P. Lillo and A. U. Acuña, *J. Photochem. Photobiol., A*, 1994, **78**, 127-138.
64. F. A. S. Chipem and G. Krishnamoorthy, *J. Phys. Chem. B*, 2013, **117**, 14079-14088.
65. A. Brenlla, M. Veiga, J. L. Pérez Lustres, M. C. Ríos Rodríguez, F. Rodríguez-Prieto and M. Mosquera, *J. Phys. Chem. B*, 2013, **117**, 884-896.
66. P. Toele and M. Glasbeek, *Chem. Phys. Lett.*, 2005, **407**, 487-492.
67. F. A. S. Chipem and G. Krishnamoorthy, *J. Phys. Chem. A*, 2009, **113**, 12063-12070.

View Article Online
DOI: 10.1039/C8CP03835J

68. F. A. S. Chipem, A. Mishra and G. Krishnamoorthy, *Phys. Chem. Chem. Phys.*, 2012, **14**, 8775-8790.
69. P. Cornago, P. Cabildo, R. M. Claramunt, L. Bouissane, E. Pinilla, M. R. Torres and J. Elguero, *New J. Chem.*, 2009, **33**, 125-135.
70. F. Tomas, J. L. M. Abboud, J. Laynez, R. Notario, L. Santos, S. O. Nilsson, J. Catalan, R. M. Claramunt and J. Elguero, *J. Am. Chem. Soc.*, 1989, **111**, 7348-7353.
71. E. D. Raczyńska, W. Kosińska, B. Ośmiałowski and R. Gawinecki, *Chem. Rev.*, 2005, **105**, 3561-3612.
72. I. B. Dzvinchuk and M. O. Lozinskii, *Chemistry of Heterocyclic Compounds*, 2011, **46**, 1454.
73. M. Pulst, H. Elgabarty, D. Sebastiani and J. Kressler, *New J. Chem.*, 2017, **41**, 1430-1435.
74. L. Lunazzi, F. Parisi and D. Macciantelli, *J. Chem. Soc. Perk. T. 2*, 1984, DOI: 10.1039/P29840001025, 1025-1028.
75. S. Trofimenko, G. P. A. Yap, F. A. Jove, R. M. Claramunt, M. Á. García, M. D. Santa Maria, I. Alkorta and J. Elguero, *Tetrahedron*, 2007, **63**, 8104-8111.
76. K. T. Potts, *Chem. Rev.*, 1961, **61**, 87-127.
77. E. Lucenti, A. Forni, C. Botta, L. Carlucci, C. Giannini, D. Marinotto, A. Previtali, S. Righetto and E. Cariati, *J. Phys. Chem. Lett.*, 2017, **8**, 1894-1898.
78. H. Bhatia, I. Bhattacharjee and D. Ray, *J. Phys. Chem. Lett.*, 2018, **9**, 3808-3813.
79. L. Yang, X. Wang, G. Zhang, X. Chen, G. Zhang and J. Jiang, *Nanoscale*, 2016, **8**, 17422-17426.
80. T. Zhang, X. Wang, Z. An, Z. Fang, Y. Zhang and W. Z. Yuan, *ChemPhysChem*, 2018, **19**, 2389-2396.

TOC Graphic

View Article Online
DOI: 10.1039/C8CP03835J